Effects of conical nozzle configuration on impulse coupling coefficient in repetitively-pulsed laser propulsion*

CAO Zheng-rui(曹正蕊)[1]**, **HONG Yan-ji**(洪延姬)[2], and **WEN Ming**(文明)[2]

1. Department of Postgraduates, the Academy of Equipment Command &Technology, Beijing 101416, China

2. Department of Basic Science, the Academy of Equipment Command &Technology, Beijing 101416, China

(Received 4 February 2009)

A dimensionless factor was introduced to deduce the analytic expression of impulse coupling coefficient for conical nozzles in the case of spherical symmetry, and a high precision impact pendulum system was used to measure impulse coupling coefficients of 15 conical nozzles with different cone angles and lengths. The expression was corrected according to experimental values. The results indicate that: 1) impulse coupling coefficient increases firstly and then decreases with augment of dimensionless length when cone angle is fixed;2) impulse coupling coefficient decreases monotonously with augment of cone angle when dimensionless length is fixed;3) it is of great importance for improving impulse coupling coefficient to increase the rate of laser energy deposition.

Document code: A **Article ID:** 1673-1905(2009)03-0190-4

DOI 10.1007/s11801-009-8213-9

The nozzle configuration exerts a direct influence on impulse coupling coefficient in an air-breathing mode of repetitively-pulsed laser propulsion. Much attention has been paid to numerical and experimental methods to develop the nozzle configuration characteristics i.e. the relationship between the impulse coupling coefficient and the nozzle configuration. A series of axisymmetric Myrabo lightcraft vehicles were propelled by air-breathing, pulsed-detonation engines with impulse coupling coefficient measured with ballistic pendulums as well as a piezoelectric load cell and fell within the range of 100-143 N/MW [1]. Ref.[2] and Ref.[3] simulated and tested linear and parabolic configurations of nozzle with and without considering the focusing system respectively. Ref.[4] investigated the wave structures of laser propulsion flow field at 3 different constraint conditions experimentally and found that the flow field expanded with a shape of ellipse at no constraint condition, while obvious reflection and diffraction of blast wave were formed at the edges under constraint conditions of plat target and 15° expanding target. From the single pulse horizontal and vertical propulsion tests, Ref.[5] and Ref.[6] came to the conclusion that with fixed caliber of the parabolic nozzle, the shorter of focus and the longer of length was, the bigger impulse coupling coefficient was. But Ref.[7] drew an oppositional conclusion that impulse coupling coefficient was bigger when the focus was shorter from simulation. It was obvious that there were some differences between experimental and numerical results. Moreover, there are some difficulties in verifying and extending these results because there was a lack of theoretical support in complex nozzle configuration performances.

Among different possible geometrical performances of nozzles, the simple conical nozzle subjected to point laser energy deposition at the apex of the cone, which corresponds to a spherically-symmetric explosion, is experimented and discussed in this paper. The impulse coupling coefficients of 15 kinds of conical nozzles with different cone angles and lengths are measured with an impact pendulum, and the theoretical results are verified and updated.

An incident beam of laser is focused by a lens and then its energy is deposited at the apex of a conical nozzle. A spherically-symmetric shock wave forms and a portion of it is within the cone, as shown in Fig.1.The propagation of shock wave can be described by the point similarity solution[8].

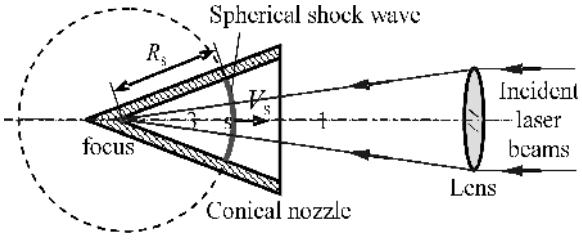

Fig.1 Sketch of conical nozzle and spherical shock wave

* This work has been supported by the National Natural Science Foundation of China (No. 10672184).

** E-mail: jessie 8007@163. com.

It is assumed that the laser effect by means of the plasma region appearing at t =0 and its initial radius equaling to 0 is modeled. The density ρ, pressure p and velocity u of disturbed gas behind the shock waves i.e. region 3 in Fig.1, can be expressed as a function of dimensionless velocity $\overline{u}$, respectively,

$$\frac{\rho}{\rho_s}=\left(\frac{-2(3\gamma-1)\overline{u}+5(\gamma+1)}{-\gamma+7}\right)^{\frac{13\gamma^2-7\gamma+12}{(3\gamma-1)(2\gamma+1)(-\gamma+2)}}\times \left(\frac{2\gamma\overline{u}-(\gamma+1)}{\gamma-1}\right)^{\frac{3}{2\gamma+1}}\left(\frac{-2\overline{u}+(\gamma+1)}{\gamma-1}\right)^{\frac{-2}{-\gamma+2}},$$

$$\frac{p}{p_s}=\left(\frac{-2(3\gamma-1)\overline{u}+5(\gamma+1)}{-\gamma+7}\right)^{\frac{13\gamma^2-7\gamma+12}{5(3\gamma-1)(-\gamma+2)}}\times \left(\frac{-2\overline{u}+(\gamma+1)}{\gamma-1}\right)^{\frac{-\gamma}{-\gamma+2}}\overline{u}^{\frac{6}{5}}, \text{ and}$$

$$\frac{u}{u_s}=\left(\frac{-2(3\gamma-1)\overline{u}+5(\gamma+1)}{-\gamma+7}\right)^{\frac{-(13\gamma^2-7\gamma+12)}{5(3\gamma-1)(2\gamma+1)}}\times \left(\frac{2\gamma\overline{u}-(\gamma+1)}{\gamma-1}\right)^{\frac{\gamma-1}{2\gamma+1}}\overline{u}^{\frac{3}{5}}, \quad (1)$$

where ρ_s, p_s and u_s represent the density, pressure and velocity immediately behind the shock wave i.e. region s in Fig.1, respectively. The expressions of them are as follows,

$$\rho_s=\frac{\gamma+1}{\gamma-1}\rho_1,$$

$$p_s=\frac{2}{\gamma+1}\rho_1 V_s^2,$$

$$\text{and } u_s=\frac{2}{\gamma+1}V_s, \quad (2)$$

where ρ_1 is the density of undisturbed gas of region 1 in Fig.1; and V_s is the propagation velocity of the shock wave.

The propagation velocity V_s and position R_s of the shock wave can be expressed as:

$$V_s=\left(\frac{4E_{in}\eta(\gamma+1)(\gamma-1)}{125\rho_1\omega I_1}\right)^{\frac{1}{5}}t^{-\frac{3}{5}}, \text{ and}$$

$$R_s=\left(\frac{25E_{in}\eta(\gamma+1)(\gamma-1)}{8\rho_1\omega I_1}\right)^{\frac{1}{5}}t^{\frac{2}{5}}, \quad (3)$$

where ω is the cone solid angle and is related to the half angle θ by ω=2π(1−cosθ); R is the cone length; E_{in} is the energy of incident laser, η is the rate of laser energy deposition at the apex of the cone; and I_1 is a function of only one parameter γ,

$$I_1=\int_0^{R_s}\left(\frac{p}{p_s}+\frac{\rho}{\rho_s}\left(\frac{u}{u_s}\right)^2\right)\left(\frac{r}{R_s}\right)^2 \mathrm{d}\left(\frac{r}{R_s}\right), \quad (4)$$

where r is the distance from the conical nozzle apex.

A dimensionless factor named dimensionless length of the cone is introduced, which is defined as the ratio of the cone length R and the characteristic shock wave radius $\overline{R}$.

$$\overline{R}=\frac{R}{R^*}=\frac{R}{\left(\frac{2E_{in}\eta}{p_1(1-\cos\theta)}\right)^{\frac{1}{3}}}, \quad (5)$$

where p_1 is the pressure of undisturbed gas of region 1 in Fig.1. Suppose that the time when the shock wave arrives at the exit of the cone is t_{arr}. The impulse I in the time of 0-t_{arr} can be calculated as an integral of time-varying thrust F, and the theoretical impulse coupling coefficient C_m is expressed as,

$$C_m=\frac{I}{E_{in}}=\frac{\int_0^{t_{arr}}F\mathrm{d}t}{E_{in}}=\frac{2\pi\int_0^{t_{arr}}\int_0^{R_s}(p-p_1)r\sin^2\theta\mathrm{d}r\mathrm{d}t}{E_{in}}. \quad (6)$$

Combining formula (1)-(6), the relationship between C_m and θ, $\overline{R}$ can be given as.

$$C_m(\theta,\overline{R})=\frac{36\eta\sqrt{2\pi\gamma}(1+\cos\theta)\left(3(\gamma-1)I_2\overline{R}^{3/2}-2\pi I_1\overline{R}^{9/2}\right)}{c_1\sqrt{(\gamma+1)(\gamma-1)I_1}}, \quad (7)$$

where c_1 is the sonic gas velocity, and I_2 is a function of only one parameter γ,

$$I_2=\int_0^{R_s}\frac{p}{p_s}\left(\frac{r}{R_s}\right)\mathrm{d}\left(\frac{r}{R_s}\right). \quad (8)$$

It is obvious from formula (7) that the maximum of C_m corresponds to

$$\overline{R}=\left(\frac{(\gamma-1)I_2}{2\pi I_1}\right)^{\frac{1}{3}}, \quad (9)$$

where γ is about 1.2-1.3[9] for air and when γ=1.25, the maximum of C_m corresponds to $\bar{R}$ =0.36.

The inner surface of the conical nozzle is determined by the cone angle and length definitely. 15 kinds of different inner surfaces with the cone angle 60°, 90° and 120°, and 5 kinds of the cone length with one angle are processed. The nozzles with the same cone angle and different length are designed to a set of accessories that can be assembled. Fig.2 shows a photograph of the conical nozzle with the cone angle 120°. A pole of "L" shape and 2 blocks are used to connect the swing pole, which is a new kind of connection. A photograph of the 120° nozzle with the swing pole is shown in Fig. 2, too.

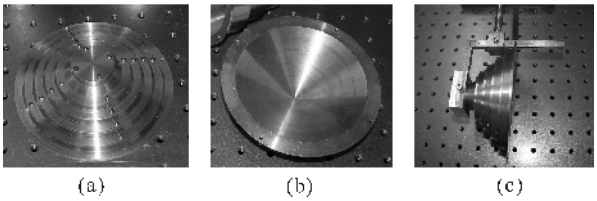

Fig.2 Photograph of conical nozzle in 120°

Fig.3 shows the experimental setup. A TEA CO_2 laser can provide up to 60 J single pulse energy. A beam of the CO_2 laser is attenuated by a silicon polishing slice before focused by a GaAs lens when expecting smaller 30 J single pulse energy, otherwise the beam is focused at position A in Fig.3 directly. The beam is focused along optical axis to make sure that the energy can deposit at the apex and the facula is as small as possible.

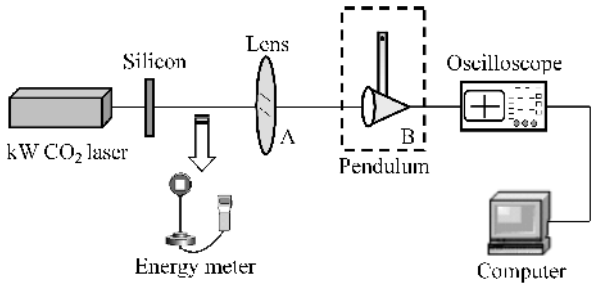

Fig.3 Sketch of experimental setup

A Ginteck-100 energy meter is parked between the slice and lens, and it is used to measure the incident laser energy before focusing in each test. The impulse is measured with a high precision impact pendulum system, which includes an incremental revolution encoder, swing poles, conical nozzles, connecting pieces and so on. The pendulum at position B in Fig.3 hangs the cone whose apex is on focus of the lens. The pulse signals output by the encoder are dealt with to gain the maximum tilt angle, and then impulse coupling coefficient can be acquired[10]. The survey accuracy of energy and impulse are both 5%. 5 tests are made repeatedly for each configuration in order to reduce the relative error.

The swing poles of 200 mm and 400 mm are used to calibrate the system parameters of each nozzle such as moment of inertia, the arm of force and natural period. While the swing pole of 200 mm is chosen to carry through impact experiments in order to gain bigger swing amplitudes. In the case of E_{in}, η, p_1 and 2θ fixed, it is obvious from formula (5) that R^* is constant in follow and one R corresponds to only one $\bar{R}$. Relationship between C_m and $\bar{R}$ when η = 50% is shown in Fig.4, in which the 3 solid lines are the fitting curves of nozzles with 3 different cone angles respectively, and the dashdotted line represents $\bar{R}$ = 0.36 (γ = 1.25) when C_m is maximum.

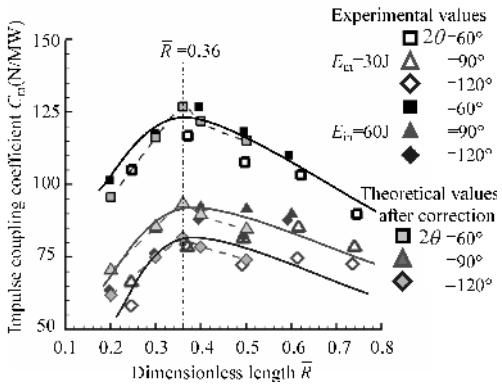

Fig.4 Impulse coupling coefficient vs. conical nozzle structure

It is can be seen from Fig.4 that 1) the experimental value of C_m falls within the range of 50-130 N/MW when 2θ is within the range of 60-120°. The magnitude of the acquired C_m is consistent with the results of an air-breathing mode in laser propulsion at present[1-7]; 2) in the case of 2θ fixed, C_m increases firstly and then decreases with the augment of $\bar{R}$ and the maximum of experimental C_m corresponds to $\bar{R}$ = 0.36, too; 3) and in the case of $\bar{R}$ fixed, C_m decreases monotonously with the augment of 2θ. All the C_m values of 2θ < 40° in Ref.[11] are bigger than gained C_m in this paper, though the incident energy and the outer surface of the cones are different. It is obvious that the latter two are consistent with the results forecasted by formula (7).

The theoretical and experimental results are the same in quality but different in quantity, and the theoretical values are higher than the experimental results because of without considering the effects of friction, heat exchange, ionization, real gas and so on inside the nozzles and ignoring the contributions of exhaust and refill stages outside the nozzles in theoretical analysis. Actually, in the case of lens focusing,

the process of laser energy deposition has a certain time scale, in which the laser supported detonation (LSD) will form and its shape is ellipsoid [12]. Different conditions of E_{in}, p_1, 2θ, R and so on influence the intensity, velocity, shape and evolvement of LSD, which induces the values of η changing. All the nozzles have η =50% under 2 incident energy in Fig.4 and it is only for an element analysis by all appearance.

Two correction coefficients of α_1 and α_2 are introduced to correct theoretical expression of C_m i.e. formula (7), one is only related with 2θ and the other with $\bar{R}$. According to experimental results, α_1 decreases with the augment of 2θ and is smaller than 1 for all 2θ, and α_2 equals to 1 approximately near $\bar{R}$ = 0.36 for the theoretical maximum of C_m. The theoretical values after correction are shown in Fig.4 too and the dashed lines are the fitting curves. It can be seen that the experimental results and the theoretical values after correction are nearly consistent not only in quality but also in quantity. Tab.1 shows the correction coefficients used in Fig.4. It can be forecasted that more and more experimental information will be got hold of with the development of experimental methods and conditions, which lays the foundation for correcting theoretical results further.

Tab.1 Correction coefficients used in Fig.4

2θ	α_1	$\bar{R}$	α_2
60°	0.46	0.2	1.3
90°	0.37	0.3-0.4	1.0
120°	0.36	0.5	3.0

A dimensionless length of conical nozzles is introduced and the relationship between impulse coupling coefficient and the cone configuration is measured. It comes to the conclusion that:

(1) Impulse coupling coefficient of conical nozzles has intimate relations with the cone angle and the dimensionless length under the effect of a single pulse laser. In the case of the cone angle fixed, impulse coupling coefficient increases firstly and then decreases with the augment of the dimensionless length and the maximum of impulse coupling coefficient corresponds to constant dimensionless length $\bar{R}_{opt}$ = 0.36 when γ=1.25. In the case of the dimensionless length fixed, impulse coupling coefficient decreases monotonously with the augment of 2θ and C_m=125 N/MW when 2θ = 60° and $\bar{R}$ = 0.36.

(2) The theoretical maximum of impulse coupling coefficient is acquired when 2θ=0° and $\bar{R}$ =0.36. $C_{m\text{-}max}$=295 N/MW when η = 50% and $C_{m\text{-}max}$=354 N/MW when η = 60%. It is manifested that improving the rate of laser energy deposition as much as possible is an effective approach to optimize the propulsion performance. The rate of deposition determined by many factors such as incident laser energy, ambient parameters, nozzle structure parameters and so on is one of the most important performance parameters in air-breathing mode of repetitively-pulsed laser propulsion and it is worthy of being paid attention to.

References

[1] L N Myrabo, D G Messitt, and F B Mead, AIAA Paper, (1998), 98.

[2] C Y Cui, Y J Hong, G Q He, Q Li, and Z R Cao, High Power Laser and Particle Beams, **18** (2006), 194 (in Chinese)

[3] C Y Cui, Y J Hong, J Wang, and G Q He, Chinese Journal of Lasers, **33** (2006), 739. (in Chinese)

[4] M Wen, Y J Hong, J F Ye, G Y Wang, and C Y Cui, Journal of Optoelectronics • Laser, **18** (2007), 1104 (in Chinese)

[5] P Gong, and Z P Tang, Explosion and Shock Waves, **23** (2003), 501 (in Chinese)

[6] Z P Tang, P Gong, X J Hu, J Cai, R Q Tan, and Y Lu, Acta Aeronautica et Astronautica Sinica, **26** (2005), 13 (in Chinese)

[7] P Gong, and Z P Tang, Second International Symposium on Beamed Energy Propulsion, 2004, 31.

[8] L I Sedov, Similarity and Dimension Methods in Mechanics. Beijing: Science Press, 1982, 235 (translated)

[9] Ya B Zel'dovich, and Yu P Raizer, Physics of Shock Waves and High-temperature Hydrodynamics Phenomena. Beijing: Science Press, 1980, 97.

[10] M Wen, Y J Hong, J H Wang, and J Wang, Chinese Journal of Scientific Instrument, **28** (2007), 140 (in Chinese)

[11] V P Ageev, A I Barchukov, F V Bunkin, V. I. Konov, V. P. Korobeinikov, B.V. Putjatin, and V. M. Mudjakov, Acta Astronautics, **7** (1980), 79.

[12] N Glumac, G Elliott, and M Boguszko, 43rd AIAA Aerospace Sciences Meeting and Exhibit, 2005, 1.